

Numerical and experimental investigations on internal flow characteristic in the impact sprinkler

Haijun Yan · Yangjun Ou · Kazuhiro Nakano · Chengbo Xu

Published online: 18 March 2009
© Springer Science + Business Media B.V. 2009

Abstract An integral 3D numerical model based on the structural characteristics of the impact sprinkler was constructed to simulate the relationship between flow rates and inlet pressures as well as the flow field distribution by computational fluid dynamics (CFD). A commonly used PY₁₄₀ sprinkler in China with three different flow straighteners in lengths of 80, 140 mm and 200 mm respectively and without flow straightener was investigated under inlet pressures ranging from 300 kPa to 500 kPa numerically and experimentally. The simulation results obtained revealed that the predicted relationship of flow rates and inlet pressures was in good agreement with the measurements. Fixing a proper flow straightener can effectively improve the turbulent flow state inside the sprinkler and lead to a more uniform velocity at the nozzle outlet. The sprinkler with a flow straightener resulted in a larger pressure loss within the internal flow than the sprinkler without flow straightener. A longer flow straightener caused a smaller turbulent kinetic energy at the nozzle outlet, which indicated that the length of flow straightener had no significant effect on the flow rate. As well, it was found that reversed flow happened near the nozzle outlet with a diffused angle of 90° could be observed clearly. The decrease of the diffused angle from 90° to 60° can supply a larger flow rate, which was verified by an experiment.

Keywords Sprinkler · Hydraulic characteristics · Turbulent flow · CFD simulation · Experiment

H. Yan (✉) · Y. Ou
College of Water Conservancy and Civil Engineering, China Agricultural University, Haidian, Beijing,
People's Republic of China
e-mail: water220@cau.edu.cn

K. Nakano
Graduate School of Science and Technology, Niigata University, Niigata, Japan

C. Xu
China Irrigation and Drainage Development Center, Beijing, People's Republic of China

Abbreviations

FS Flow Straightener
CFD Computational Fluid Dynamics

Introduction

As one of the most efficient and effective irrigation methods in agriculture, sprinkle irrigation has many remarkable advantages such as adapting to diverse terrains, field crops, soil structures and so on, supplying uniform water application and high water use efficiency and minimizing labor requirement (Keller and Bliesner 1990; Li 1995).

Sprinkler regarded as a key component in sprinkle irrigation system delivers water across the field to be irrigated at a given working pressure. In general, hydraulic characteristics of an individual sprinkler have a great influence on the overall quality of irrigation system. Thus developing a sprinkler with more excellent hydraulic properties has always been focused by researchers. Since the invention of the sprinkler, enormous efforts have been made on the external flow characteristics in terms of flow rate, radius, application rate, water distribution profile, etc. And a variety of research achievements and proposals relative to the hydraulic characteristic of sprinkler have been offered in open literature (Kincaid 1982; Kincaid 1991; Kincaid et al. 1996; Sourell et al. 2003).

It is well known that the traditional procedure of designing a new sprinkler can be roughly divided into four steps: structure design, manufacture, assembling and experiment. Some steps are also important for improvement on the sprinkler's performance. This developing cycle is very time-consuming and expensive. Additionally, due to the difficulty in testing internal flow fields of the sprinkler, traditional experiments conducted are mainly confined to the external hydraulic characteristics. Therefore relevant studies on the sprinkler's internal flow characteristics have seldom been reported in public. In fact, the sprinkler's external hydraulic performance depends primarily on the geometric parameters of the internal flow regime. Generally speaking, as water flows through an entity with smoother boundaries, a smaller pressure loss and more uniform flow velocities at the nozzle outlet can be offered, which benefits the external hydraulic performance. The impact sprinkler considered as the most widely used rotary sprinklers in the world consists of bearing nipple, bend, tube and one or two nozzles. For a medium or high pressure impact sprinkler, a unique flow straightener (FS) is usually required inside tube in order to improve the internal flow turbulence. The relative experiments employed revealed that a proper flow straightener can greatly affect on the external hydraulic characteristics. In addition, as the length of the flow straightener increases, the radius of the sprinkler will be increased somewhat (Li 1995).

Computational fluid dynamics (CFD) approach has been utilized to simulate and visualize internal flow regimes in a wide range of application fields such as industry, aeronautics, petroleum and agriculture (Chen et al. 2006; Novozhilov et al. 1997; Renn and Hsiao 2004). Up to now, CFD technique has been successfully applied in designing and developing irrigation devices including hydro cyclone filters, pipe junctions, emitters, etc. Several papers on CFD simulation of agricultural devices mentioned above have been published since the year of 2000 (Li et al. 2005; Palau et al. 2004; Wei et al. 2006; Xu et al. 2006; Zhang et al. 2007). However, valuable papers on agricultural sprinklers are seldom available. Yuan et al. (2005) applied CFD technology to calculate the relationship between flow rates and working pressures, and to predict the special position of lean-wall of complete fluidic sprinkler as well. However they only employed one turbulence model and made no comparisons of computational parameters in detail. Li and Wang (2006) indicated

that the flow straightener has an effect on the pressure loss inside the sprinkler using the ANSYS software. But their computational domain used was not complete and the simulated results were not verified experimentally.

Hence, this paper aims to model a typical internal flow passage of impact sprinkler with and without flow straightener and to conduct a numerical simulation on the internal flow characteristics using commercial CFD program Fluent 6.2, and then relevant experiments are to be designed to verify the accuracy of simulation.

Materials and methods

Geometric model and grid generation

Figure 1 shows a typical geometric model of the PY₁₄₀ impact sprinkler used in the simulation. During the construction of the computational domain, the surface of the internal flow regime was simplified and considered to be connected continuously. The inlet

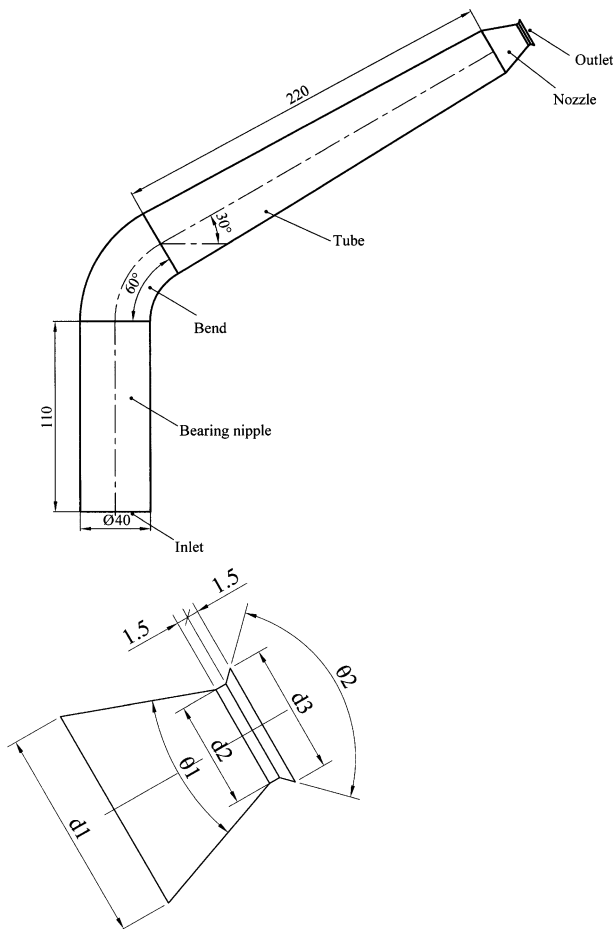
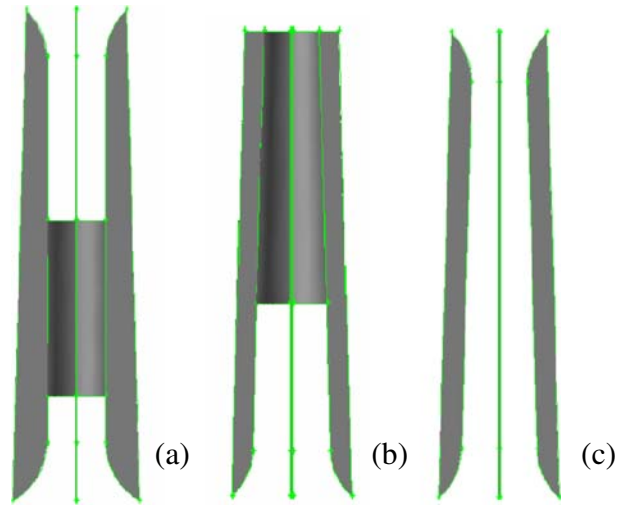


Fig. 1 A 2D model of the PY₁₄₀ sprinkler: **a** The whole internal flow regime; **b** The nozzle structure

Fig. 2 Geometric models of flow straightener: **a** FS-1 type; **b** FS-2 type; **c** FS-3 type



diameter of the geometric model is 40 mm and the values of the d_1 , d_2 , d_3 , θ_1 and θ_2 of the nozzle are 28 mm, 14 mm, 17 mm, 40° and 90° , respectively. The value of d_2 is commonly selected as the nominal diameter of the nozzle. In order to obtain different hydraulic characteristics of the studied sprinkler, five nozzle diameters as 12 mm, 13 mm, 14 mm, 15 mm and 16 mm were employed. The magnified drawing of the nozzle is depicted in Fig. 1b.

Two typical flow straighteners used for flow improvement were called FS-1 and FS-2 types respectively, as illustrated in Fig. 2a and b. Both two flow straighteners were composed of four circumferentially positioned vanes and a conical or circular cylinder. The radial width of the vane along the axial line was variable for FS-1, while kept constant for FS-2. Both FS-1 and FS-2 types were manufactured in the first stage and then inserted into the tube during the assembling stage. In addition, another type of flow straightener named FS-3 was compared as well, shown in Fig. 2c. All four vanes of FS-3 were the same to those of FS-2. The vanes, conical tube or circular cylinder were made with a 0.5-mm thickness sheet iron. In order to compare the effect of different lengths on the flow characteristics, three lengths of 80 mm, 140 mm and 200 mm were investigated, respectively. The FS-1 type with length of 80 mm was described as FS-1-80. The description method can be suitable for other geometric models except the case of sprinkler without flow straightener (called as No FS). In total, ten cases of computational models were investigated in this study.

Grid selection is an important technique to improve the accuracy of the solutions in numerical simulation. In order to ensure accuracy of the calculations, a preliminary grid dependence study was performed. Simulations were carried out by using different mesh grids. In general, a multi-block technique can be used to effectively split the whole internal flow region into several sub-domains. For sprinkler without flow straightener, the computational domain can successfully be meshed with structured or unstructured grids. As for sprinkler with flow straightener, the computational domain becomes more complex and difficult to be meshed with structured mesh grids. In this study, two unstructured mesh methods were attempted as hex/wedge elements with cooper type and tet/hybrid elements with tgrid type. The simulated deviation error from the experimental results was up to 18% for the former, while 13% for the latter. In addition, the simulated flow field in the specific

curvature by the latter approach was in better accord with the practical phenomena. In a consequence, the latter method of mesh grid generation was utilized in this simulation. In order to get high quality grids, the interval sizes of grid became smaller with the reduction in the cross-sectional area from the inlet to the nozzle outlet. As a result, the whole computational domain was meshed into tetrahedral cells in excess of 60,000 for all models.

Mathematical model

The water flowing through the sprinkler is assumed to be viscous and incompressible at normal temperature. As water goes into the inlet of the sprinkler at an economic velocity from 2 m/s to 2.5 m/s, the Reynolds number varies 0.8×10^5 to 10^5 greatly exceeding 2,300. Therefore the internal flow can be considered as fully developed turbulent flow.

The mathematical model used in this work is based on the 3-D Navier-Stokes equations (Versteeg and Malalasekera 1995). In the past decades, various numerical simulation methods including direct numerical simulation and non-direct numerical simulation have been proposed for solving the 3-D turbulent flow. It is noted that the Reynolds-Averaged Navier-Stokes (RANS) equations as one of non-direct numerical simulation methods, is the most widely used approach in turbulent flow simulation. Of all models of RANS equations, two equation turbulence models seem to be applied most widely (Ferziger and Peric 1996; Wang 2004). The preliminary comparison of three basic turbulence models of two equation models as standard $k-\varepsilon$, RNG $k-\varepsilon$ and realizable $k-\varepsilon$ indicated that the computational deviation error from the measured results by RNG $k-\varepsilon$ model is the smallest. In addition, the RNG $k-\varepsilon$ model can perform much better for a bended pipe than the other two models as described in many literatures. Hence, the RNG $k-\varepsilon$ model was eventually applied in this study. And the k and ε equations are given as follows:

k equation

$$\frac{\partial(\rho k u_i)}{\partial x_i} = \frac{\partial}{\partial x_j} \left[\alpha_k \alpha_k \mu_{eff} \frac{\partial k}{\partial x_j} \right] + G_k + \rho \varepsilon$$

ε equation

$$\frac{\partial(\rho \varepsilon u_i)}{\partial x_i} = \frac{\partial}{\partial x_j} \left[\alpha_\varepsilon \mu_{eff} \frac{\partial \varepsilon}{\partial x_j} \right] + \frac{\varepsilon}{k} \left(C_{1\varepsilon}^* G_k - C_{2\varepsilon} \rho \varepsilon \right)$$

Where

$$\begin{aligned} \mu_{eff} &= \mu + \mu_t \\ \mu_t &= \rho C_\mu \frac{k^2}{\varepsilon} \\ C_{1\varepsilon}^* &= C_{1\varepsilon} - \frac{\eta(1 - \eta/\eta_0)}{1 + \beta\eta^3} \\ \eta &= (2E_{ij} \cdot E_{ij})^{1/2} \frac{k}{\varepsilon} \\ E_{ij} &= \frac{1}{2} \left(\frac{\partial u_i}{\partial x_j} + \frac{\partial u_j}{\partial x_i} \right) \end{aligned}$$

In these equations, k is the turbulent kinetic energy, ε the rate of dissipation, $u = u\vec{i} + v\vec{j} + w\vec{k}$ where u , v , w the velocity in direction of x , y , z , respectively, p the pressure, ρ the fluid density, μ the fluid viscosity, and C_μ , $C_{1\varepsilon}$, $C_{2\varepsilon}$, α_k , α_ε , η_0 , and β are the

corresponding coefficients as proposed by Yakhot and Orzag (1986): $C_\mu=0.0845$, $C_{1\varepsilon}=1.42$, $C_{2\varepsilon}=1.68$, $\alpha_k=\alpha_\varepsilon=1.39$, $\eta_0=4.377$ and $\beta=0.012$.

Boundary conditions and numerical method

In this simulation, inlet pressures as 300 kPa, 350 kPa, 400 kPa, 450 kPa and 500 kPa were implemented respectively. Because of water discharged directly into the air, the outlet of the sprinkler was treated as standard atmosphere. The computational surface roughness was not valuably considered and the wall of calculation region assumed to be under no-slip condition. In near-wall treatment, three kinds of methods as Standard wall functions, Non-equilibrium wall functions and Enhanced wall treatment are available. Almost no significant difference of the simulated results by three methods for FS-1-140 was found. Due to the first method requiring less computation time and iteration steps compared with the latter two methods, it was ultimately implemented. The continuity and 3-D Navier-Stokes equations were solved by using the SIMPLE Consistent (SIMPLEC) algorithm proposed by Van Doormal and Raithby (1984) with a segregated solver. The discretizations of the flow momentum, k and ε equations were dealt with second order upwind scheme. The y^+ value was always controlled within the recommended range less than 200. Additionally, the effect of gravity was considered in all simulations.

Experimental set-ups and procedures

The relationship between flow rates and inlet pressures regarded as a significant parameter in irrigation system design plays an important role in evaluating the performance of the sprinkler. According to the standard of ASAE S 398.1 (ASAE S398.1 2001), an experimental setup was constructed as shown in Fig. 3. Water was pressurized from the

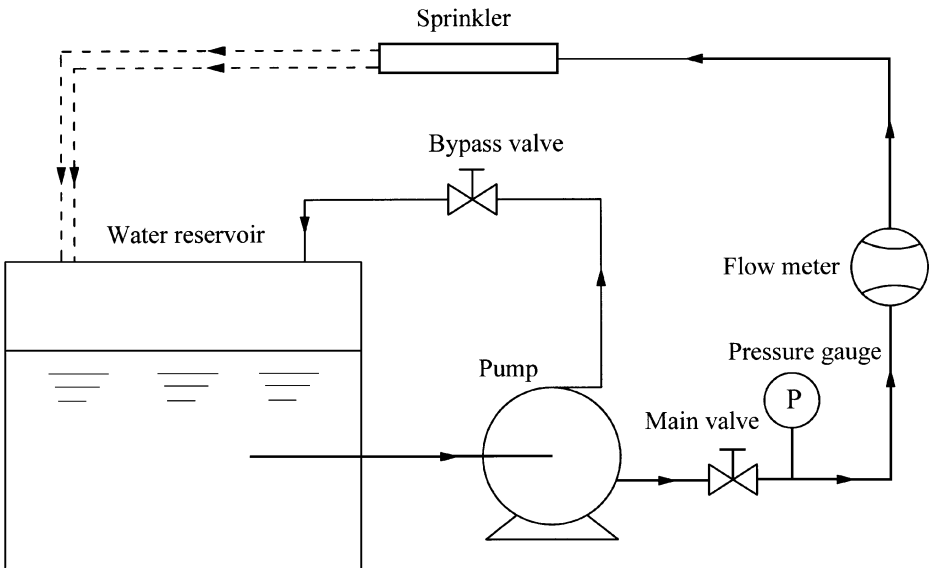
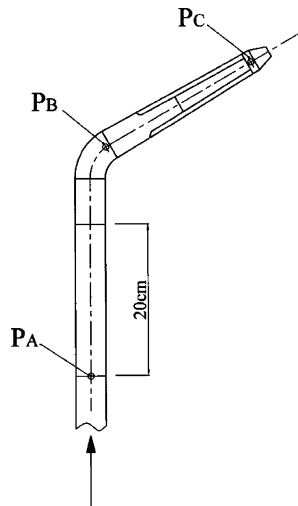


Fig. 3 Schematic diagram of experimental set-up

Fig. 4 Schematic of the pressure measurements



reservoir by a multi-stage centrifugal pump (Model: 65DL-5). An electromagnetic flowmeter (Model:E-mag DN40) located between the control valve and the tested sprinkler was used for measurement of the sprinkler's flow rate. Three static pressures as P_A , P_B and P_C were tested by pressure sensors (Model: MPM4760) as shown in Fig. 4. One pressure sensor located at 20 cm upstream the inlet of sprinkler was used to measure inlet pressure P_A . Other two pressure sensors were situated at the beginning end of the tube and just 5 mm upstream the other end of the tube for measurement of P_B and nozzle pressure P_C , respectively. The test was conducted at the experimental hall in China Agricultural University. Due to the wetted coverage area of PY₁₄₀ sprinkler larger than the space allowed for use, the water jet from the nozzle was blocked by a metal cover above the sprinkler so as to ensure water flow back into the reservoir, which was depicted in double dashed line illustrated in Fig. 3. The test sprinkler was assembled on a vertical pipe.

Table 1 Comparison of the simulated and measured flow rates

| Type | Flow rate | Inlet pressure (kPa) | | | | |
|----------|------------------------------------|----------------------|-------|-------|-------|-------|
| | | 300 | 350 | 400 | 450 | 500 |
| FS-1-140 | Measured data (m ³ /h) | 12.15 | 13.27 | 14.1 | 15.04 | 15.77 |
| | Simulated data (m ³ /h) | 13.76 | 14.88 | 15.89 | 16.85 | 17.77 |
| | Deviation error (%) | 13.2 | 12.1 | 12.7 | 12.1 | 12.7 |
| FS-2-140 | Measured data (m ³ /h) | 12.18 | 13.24 | 14.09 | 14.94 | 15.62 |
| | Simulated data (m ³ /h) | 13.72 | 14.83 | 15.84 | 16.79 | 17.74 |
| | Deviation error (%) | 12.6 | 12.0 | 12.4 | 12.4 | 13.5 |
| FS-3-140 | Simulated data (m ³ /h) | 13.82 | 14.91 | 15.99 | 16.93 | 17.81 |
| No FS | Measured data (m ³ /h) | 12.30 | 13.28 | 14.09 | 14.94 | 15.74 |
| | Simulated data (m ³ /h) | 13.83 | 14.94 | 15.94 | 16.94 | 17.89 |
| | Deviation error (%) | 12.4 | 12.5 | 13.1 | 13.4 | 13.6 |

Results and discussion

Relationship of flow rates and inlet pressures

For a sprinkler with a given nozzle diameter, the flow rate increases with the inlet pressure. The simulated flow rates for sprinklers with three kinds of flow straighteners and without flow straightener as well were compared with the experimental data. The results are shown in Table 1. Because of lack of the experimental data, the comparison for FS-3-140 was not made. For all cases, the simulated flow rates were larger than the experimental data, with a deviation error ranging from 12% to 13.6%. For each case, the deviation errors under different inlet pressures varied slightly, which indicated that the predicted relationship of flow rates and inlet pressures is in good agreement with the measured results.

The deviation error may result from the following two reasons. Firstly, the simplified computational domain assumed continuous is different from the practical model. The Second one is that surface roughness of the computational domain was not considered in the simulation.

In addition, the effect of length of the flow straightener on the simulated flow rates was also investigated. As shown in Fig. 5, the simulated results for FS-2 revealed that as the length of flow straightener increases, no apparent changes in flow rate could be observed for both simulation and measurement, which indicated that the length of the flow straightener has no significant effect on the flow rates.

Pressure distribution

The pressure distribution within the internal flow regime can be visualized by CFD simulation. Figure 6 shows the numerical contours of static pressures in a slice of $z=0.001$ m offset the central plane at inlet pressure of 400 kPa for FS-1-140. The magnitude of simulated static pressure is depicted in different colors. Most of the radial static pressures are approximately axisymmetric in the straight sections. But great pressure change occurs near the bend section where the static pressure on the convex side is higher than that on the concave side. The pressure difference between these two sides leads to transverse flow and worse turbulent flow. The minimum static pressure happens near the smallest cross-sectional area of the nozzle with a diffused angle.

Fig. 5 Comparison of simulated and measured flow rates versus inlet pressures for sprinkler with FS-2 type

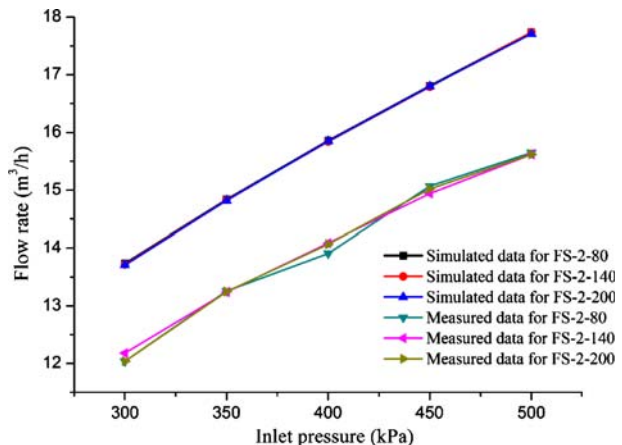
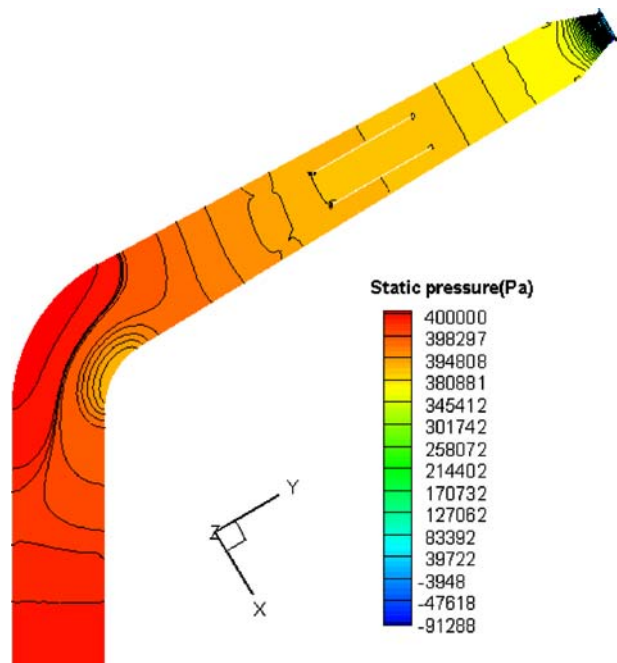


Fig. 6 Contour of static pressures for sprinkler with FS-1-140 type in a slice of $z=0.001$ m at inlet pressure of 400 kPa



In order to verify the accuracy of the pressure simulation, the simulated pressures were compared with the measured results under different inlet pressures. Figure 7 gives the static pressure distributions for FS-1-140 at inlet pressures of 300 kPa, 350 kPa and 400 kPa respectively. It can be seen that the pressure drop from the inlet of the sprinkler to the nozzle inlet varies slightly because of the small changes in cross-sectional area. But static pressure changes greatly at the nozzle with a sharply variable cross-section area. The maximum error of the simulated and measured pressures was less than 3% for all cases. In consequence, the accuracy of the numerical computation is satisfactory.

Fig. 7 Static pressure distribution from inlet to nozzle outlet for sprinkler with FS-1-140 type

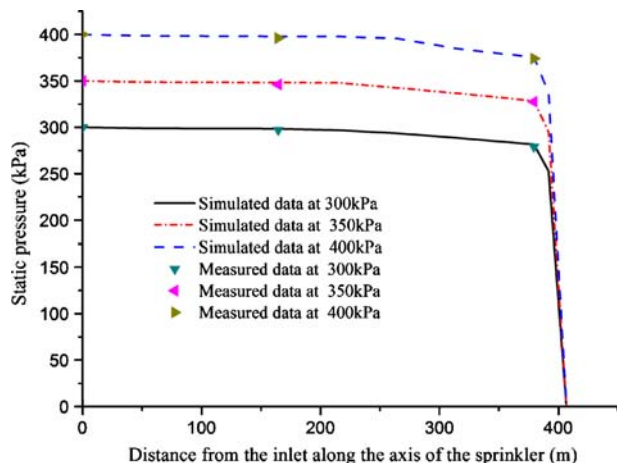
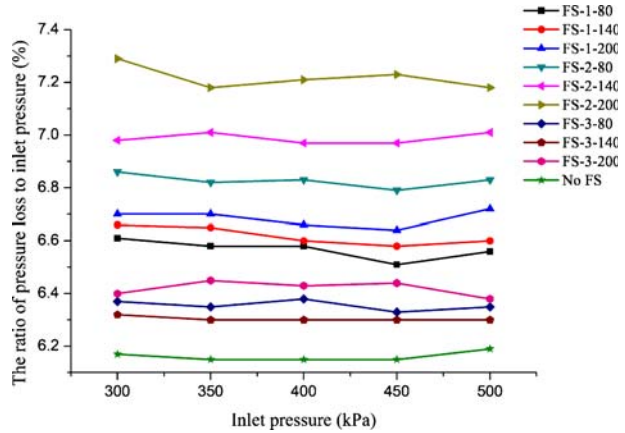


Fig. 8 The ratio of simulated pressure loss to inlet pressure versus inlet pressure for sprinkler with and without flow straightener

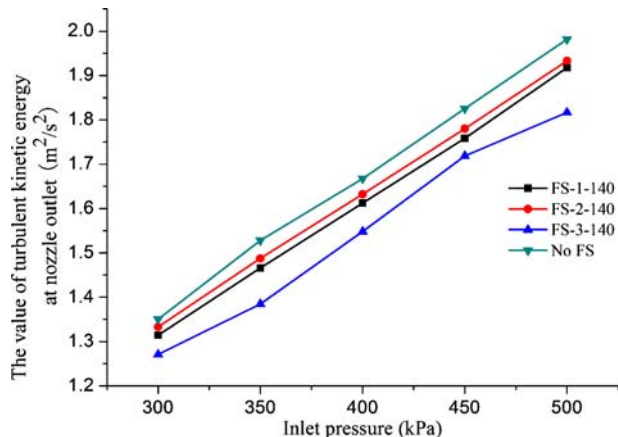


Furthermore, the effects of geometric structure of flow straightener on the pressure loss were also investigated. In this study, the term of pressure loss was defined as the difference of the inlet pressure and the nozzle pressure. Figure 8 shows some change curves of the ratio of simulated pressure loss to inlet pressure. The minimum ratio referring to the case of no flow straightener indicated that fixing flow straightener would cause some extra pressure loss inside the sprinkler. For a sprinkler with a given flow straightener, the pressure loss increases with an increasing the length of flow straightener. Of three flow straighteners studied, the FS-2 type resulted in the largest pressure loss.

Turbulent kinetic energy

The magnitude of turbulent kinetic energy at the nozzle outlet is commonly regarded as an important index in evaluation of the flow field. The lower the turbulent kinetic energy is, the larger throw distance the sprinkler can supply. For cases of FS-1-140, FS-2-140, FS-3-140 and No FS, the relationships between the simulated turbulent kinetic energy at nozzle outlet versus inlet pressure are given in Fig. 9. For a particular flow straightener, the magnitude of turbulent kinetic energy increases with the increasing of the inlet pressure,

Fig. 9 The value of turbulent kinetic energy at nozzle outlet versus inlet pressure for sprinkler with and without flow straightener



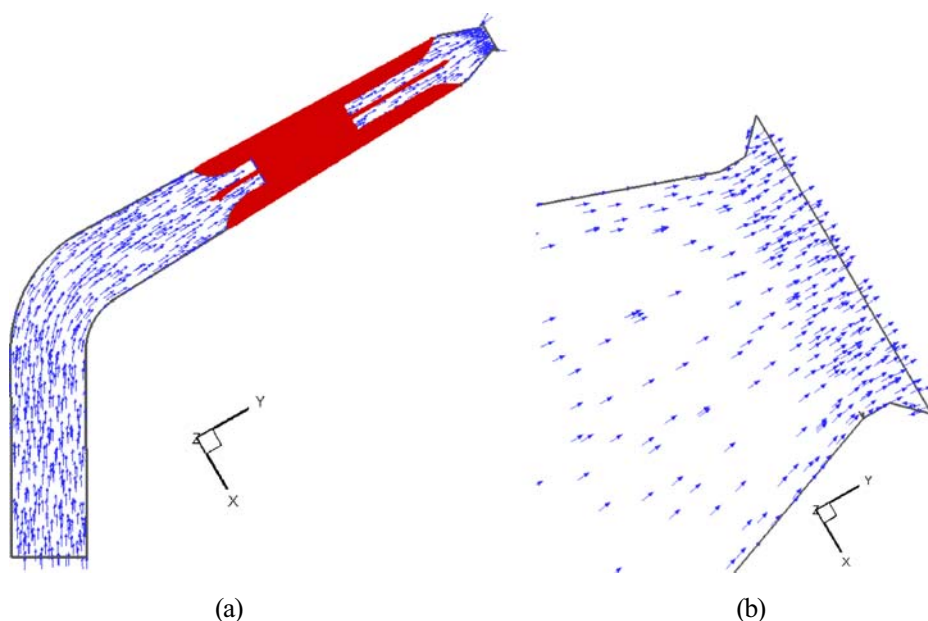


Fig. 10 Vector distributions for sprinkler with FS-1-140 type at inlet pressure of 400 kPa: **a** The whole computational domain; **b** Part of the nozzle

which means that higher inlet pressure may bring about a more turbulent flow. The simulated turbulent kinetic energy for case of No FS was larger than those for cases with flow straighteners, which indicated that fixing flow straightener can effectively improve the internal turbulence. Among three flow straighteners, the type of FS-3 is considered as the most appropriate structure due to its simulated minimum magnitude of turbulent kinetic energy. In addition, several comparisons with different lengths of flow straighteners were performed. The results showed that the turbulence kinetic energy slightly decreases with the increase of the length of flow straightener.

Visualization of the flowfield

Visualization of an instantaneous flow solution can provide some spatial information about the internal flow field. Figure 10 shows the whole velocity vectors at $z=0$ plane of the sprinkler. The internal flow appears to be in a gentle state without any strong vortex as a whole. However, the flow pattern in the region near the nozzle outlet is quite complex. Some apparent reversed flows occur around the nozzle's diffused section by reasons of the abrupt diffused angle θ_2 shown in Fig. 1b. Meanwhile, some minor transverse flows can be observed. Technically speaking, the diffused section is an important parameter in sprinkler's design. A proper diffused angle can make sprinkler deliver a larger flow rate and more uniform water distribution. On the other hand, the diffused angle may result in more reversed flows. In a general, a larger diffused angle leads to a stronger reversed flow. The simulation results showed that as the diffused angles decreased from 90° to 60° , the magnitude of the turbulent kinetic energy reduced from $1.618 \text{ m}^2/\text{s}^2$ to $1.51 \text{ m}^2/\text{s}^2$, respectively. It is noted that the drop of turbulent kinetic energy can contribute to a larger flow rate, which was verified well by an experiment that measured flow rate was larger for

angle 60° than for angle 90°, with an increase of 1.74%. It can be concluded that structural optimization approach can be effectively implemented by CFD simulation.

Conclusions

In this paper, we have conducted some numerical simulations on the agricultural sprinkler with and without flow straightener, and then carried out the experiments on the flow rate-pressure relationship and other primary pressures to verify the calculation. The following conclusions are made from the results of this study.

- 1) CFD analysis technology is suitable for designing and optimizing the geometric parameters of sprinkler, and the research cost and cycle can be greatly reduced. The predicted flow rates were 12.7% larger, on average, than the measured one under different inlet pressures for all studied cases. The change tendency of flow rates versus inlet pressures is in good agreement with the measured results.
- 2) According to the simulated results, fixing a proper flow straightener can improve the internal turbulent flow of the sprinkler and result in a more uniform velocity at the nozzle outlet. However, the flow straightener caused a larger pressure loss compared with the case without flow straightener. The maximum error between the simulated and measured pressure loss was less than 3% for all cases. In addition, the length increase of flow straightener caused a slight drop in turbulent kinetic energy at the nozzle outlet, and a moderate increase of pressure loss as well. In consequence, the increase of length had no apparent effect on the flow rate.
- 3) Visualization of the instantaneous flow fields using by CFD simulation can be useful for improvement and optimization of structural parameters of the sprinkler.

Acknowledgements The authors are greatly indebted to the National Natural Science Foundation of China (No. 50509024), Program for Young Researcher in China Agricultural University (2005031) and Program for Changjiang Scholars and Innovative Research Team in University (IRT0657). We furthermore like to thank Peter Emmanuel Ndajah for his valuable comments on writing in English.

References

- ASAE S398.1 (2001) Procedure for Sprinkler Testing and Performance Reporting, St. Joseph, Michigan
- Chen W, Wong K, Huang C (2006) A parameter study on the laminar flow in an alternating horizontal or vertical oval cross-section pipe with computational fluid dynamics. *Int J Heat Mass Transfer* 49:287–296. doi:10.1016/j.ijheatmasstransfer.2005.07.005
- Ferziger J, Peric M (1996) Computational methods for fluid dynamics. Springer, New York
- Keller J, Bliensner RD (1990) Sprinkler and trickle irrigation. Reinhold, New York
- Kincaid DC (1982) Sprinkler pattern radius. *Trans ASAE* 25(6):1668–1672
- Kincaid DC (1991) Impact sprinkler pattern modification. *Trans ASAE* 34(6):2397–2403
- Kincaid DC, Solomon KH, Oliphant JC (1996) Drop size distributions for irrigation sprinklers. *Trans ASAE* 39(3):839–845
- Li S (1995) Theory and design of sprinklers. Bingqi Industrial, Beijing
- Li P, Wang H (2006) The numerical simulation calculation to the influence of the water power losing of the regulator to the impact-drive sprinkler head. *Agric Mechanization Stud* 11:67–69
- Li Y, Li G, Qiu X et al (2005) Modelling of hydraulic characteristics through labyrinth emitter in drip irrigation using computational fluid dynamics. *Trans CSAE* 21(3):12–16
- Novozhilov V, Harvie DJE, Kent JH et al (1997) A computational fluid dynamics study of wood fire extinguishment by water sprinkler. *Fire Saf J* 29:259–282. doi:10.1016/S0379-7112(97)00027-1

- Palau SG, Arviza VG, Bralts VF (2004) Hydraulic flow behavior through an in-line emitter labyrinth using CFD techniques. ASAE/CSAE Meeting Paper, 1–8
- Renn J, Hsiao C (2004) Experimental and CFD study on the mass flow-rate characteristic of gas through orifice-type restrictor in aerostatic bearings. *Tribology Int* 37:309–315. doi:[10.1016/j.triboint.2003.10.003](https://doi.org/10.1016/j.triboint.2003.10.003)
- Sourell H, Faci J, Playan E (2003) Performance of rotating spray plate sprinklers in indoor experiments. *J Irrig Drain Eng* 129(5):376–380. doi:[10.1061/\(ASCE\)0733-9437\(2003\)129:5\(376\)](https://doi.org/10.1061/(ASCE)0733-9437(2003)129:5(376))
- Van Doormal JP, Raithby GG (1984) Enhancement of the SIMPLE method for predicting incompressible fluid flows. *Numer Heat Transf* 7:147–163. doi:[10.1080/01495728408961817](https://doi.org/10.1080/01495728408961817)
- Versteeg HK, Malalasekera W (1995) *An Introduction to computational fluid dynamics: the finite volume method*. Wiley, New York
- Wang F (2004) *analysis of computational fluid dynamics: Principles and applications of CFD software*. Tsinghua University Press, Beijing
- Wei Q, Shi Y, Dong W et al (2006) Study on hydraulic performance of drip emitters by computational fluid dynamics. *Agric Water Manage* 84:130–136. doi:[10.1016/j.agwat.2006.01.016](https://doi.org/10.1016/j.agwat.2006.01.016)
- Xu S, Zhu H, Zhang B (2006) Numerical simulation of solid-liquid separation for a hydrocyclone. *China Petrol Machinery* 34(3):24–27
- Yakhot V, Orzag SA (1986) Renormalization group analysis of turbulence: basic theory. *J Sci Comput* 1:3–11. doi:[10.1007/BF01061452](https://doi.org/10.1007/BF01061452)
- Yuan S, Zhu X, Li H et al (2005) Numerical simulation of inner flow for complete fluidic sprinkler using computational fluid dynamics. *Trans CSAM* 36(10):46–49
- Zhang J, Zhao W, Wei Z et al (2007) Numerical and experimental study on hydraulic performance of emitters with arc labyrinth channels. *Comput Electron Agric* 56:120–129. doi:[10.1016/j.compag.2007.01.007](https://doi.org/10.1016/j.compag.2007.01.007)